An optical microfluidic platform for spatiotemporal biofilm treatment monitoring

2016 J. Micromech. Microeng. 26 015013

(http://iopscience.iop.org/0960-1317/26/1/015013)

IOP Publishing Journal of Micromechanics and Microengineering

J. Micromech. Microeng. **26** (2016) 015013 (12pp) doi:10.1088/0960-1317/26/1/015013

An optical microfluidic platform for spatiotemporal biofilm treatment monitoring

Young Wook Kim[1,2,4], Matthew P Mosteller[1,4], Sowmya Subramanian[1,2], Mariana T Meyer[1,3], William E Bentley[3] and Reza Ghodssi[1,2,3]

[1] MEMS Sensors and Actuators Laboratory, Institute for Systems Research, 2173 A.V. Williams Bldg, College Park, MD 20742, USA
[2] Department of Electrical and Computer Engineering, University of Maryland, College Park, MD 20742, USA
[3] Fischell Department of Bioengineering, University of Maryland, College Park, MD 20742, USA

E-mail: kywooks@gmail.com and ghodssi@umd.edu

Received 13 July 2015, revised 9 November 2015
Accepted for publication 16 November 2015
Published 14 December 2015

Abstract

Bacterial biofilms constitute in excess of 65% of clinical microbial infections, with the antibiotic treatment of biofilm infections posing a unique challenge due to their high antibiotic tolerance. Recent studies performed in our group have demonstrated that a bioelectric effect featuring low-intensity electric signals combined with antibiotics can significantly improve the efficacy of biofilm treatment. In this work, we demonstrate the bioelectric effect using sub-micron thick planar electrodes in a microfluidic device. This is critical in efforts to develop microsystems for clinical biofilm infection management, including both *in vivo* and *in vitro* applications. Adaptation of the method to the microscale, for example, can enable the development of localized biofilm infection treatment using microfabricated medical devices, while augmenting existing capabilities to perform biofilm management beyond the clinical realm. Furthermore, due to scale-down of the system, the voltage requirement for inducing the electric field is reduced further below the media electrolysis threshold. Enhanced biofilm treatment using the bioelectric effect in the developed microfluidic device elicited a 56% greater reduction in viable cell density and 26% further decrease in biomass growth compared to traditional antibiotic therapy. This biofilm treatment efficacy, demonstrated in a micro-scale device and utilizing biocompatible voltage ranges, encourages the use of this method for future clinical biofilm treatment applications.

Keywords: bacterial biofilms, bioelectric effect, optical sensors, microfluidics

(Some figures may appear in colour only in the online journal)

1. Introduction

Bacterial biofilms are comprised of diverse communities of bacteria within an extracellular matrix that limits molecular diffusion within the biofilm, contributing to a need for higher doses of antibiotics for effective treatment [1–9]. In addition, since bacteria in biofilm structures can readily exchange genes, including those that promote antibiotic resistance, biofilms often develop higher resistivity to antibiotics compared to planktonic bacteria [4–6, 10–12]. Thus, once biofilms are established, they can incite harmful and recalcitrant infections often requiring between 500 and 5000 times greater concentrations of antibiotics for effective treatment compared to bacteria in suspension [1–3, 10–16]. As a result, the development of highly effective biofilm treatment methods utilizing sustainable levels of antibiotics is a principal driver in the development of new cures for biofilm infections [1–3, 6–9].

A combinatorial biofilm treatment method using electric fields in the presence of antibiotics has been demonstrated previously, showing enhanced treatment efficacy under reduced antibiotic dosages [17–26]. This phenomenon, known as the bioelectric effect (BE), uses traditional biocides in conjunction with direct or alternating current (DC or AC) electric fields [17–19, 21–26]. One of the prominent hypotheses on the

[4] These authors contributed equally to this work.

application of DC electric fields is that it induces electrophoresis and non-uniform electrolyte distributions within biofilms as well as their surrounding media [19–24]. The induced electrolyte concentration gradients and byproducts generated as a result of the electrolysis of the surrounding media impose metabolic stresses on the bacteria in biofilms, including local pH changes, oxygen depletion, and increased electrochemical reactivity [19, 20, 22–24]. Biofilm treatment efficacy can be improved dramatically when antibiotics are introduced simultaneously with electrically induced environmental modifications, such as the bioelectric effect [17–21, 24]. Conversely, it is suggested that the presence of an alternating current (AC) electric field induces increased biofilm permeability due to local molecular vibrations within the extracellular matrix [19, 27–29]. The AC electric field applies alternating electrostatic forces to the partially charged molecules within biofilms, thereby making them more susceptible to the effects of antibiotics [25–29]. When such an induced biofilm permeability condition is combined with antibiotics, the diffusion rate of the drugs within the biofilm is enhanced, resulting in increased treatment efficacy [19, 25, 26]. However, detailed investigations of the exact mechanism of the BE are still ongoing.

Although previous work has shown effective biofilm treatment via the BE, biocompatible treatment methods utilizing voltages below the threshold of biological fluid electrolysis [27] have not been demonstrated [17–21, 23, 25]. Typical electric field intensities demonstrating effective biofilm treatment by the BE have been reported in the range of 2.0–5.0 V cm^{-1}, corresponding to voltage potentials of 0.8–2.0 V in traditional cuvette apparatuses [17–21, 24, 26, 30] based on the linear relation between electric field and voltage potential for a given electrode spacing [29]. Such voltages are higher than the standard electrolysis potential of biological fluids (~0.82 V at 25 °C, pH 7) [27], resulting in the generation of harmful radical ions and rendering these treatments incompatible for clinical applications. To address this shortcoming in meso-scale systems, voltages below the electrolysis threshold are required. However, efficacy of the bioelectric effect is reduced significantly when decreased electric field intensities are applied [17–21, 24, 26]. As a result, the high voltages required for strong electric field induction, and thus significant BE efficacy, have posed a consistent challenge for utilizing the BE in meso-scale clinical applications.

Recent work in our group has demonstrated a bioelectric effect that is capable of efficient biofilm treatment requiring voltages well below the media electrolysis potential [28, 29]. We demonstrated that the major factor contributing to the enhancement of the BE treatment efficacy was the total electrical energy applied to the biofilms [29]. The electrical potentials, provided by either the AC and/or DC signals were significantly smaller than the bulk media electrolysis potential used in previously reported studies of the BE [17–21, 24–26]. Application of different types of electrical signals of similar energies in combination with the antibiotic gentamicin (10 μg ml^{-1}) revealed equivalent reduction of viable *Escherichia coli (E. Coli)* K-12 W3110 biofilms in a traditional macro-scale setup [29]. Additionally, a linear relationship between the energy of the applied electrical signal and the treatment efficacy of the BE was demonstrated [29]. We have also demonstrated real-time micro-scale detection of biofilm growth and inhibition when treated with the BE, using an integrated surface-acoustic-wave (SAW) microsystem [31] .

We have previously reported on the system-level design and modeling of a microfluidic biofilm observation, analysis and treatment (Micro-BOAT) platform [32]. In this work, we utilize this platform to demonstrate the BE on-chip with voltages lower than the electrolysis threshold. Scaling of the BE to the micro-scale is a critical requirement in realizing the treatment for *in vivo* and *in vitro* biofilm infection management. Not only does this ensure the use of biocompatible parameters, including reduced voltages, it moreover offers advantages of high experimental throughput, decreased volume, and precise environmental control within microfluidic growth environments [33–38]. The Micro-BOAT platform developed is capable of real-time biofilm monitoring within a microfluidic system and enables both quantitative and qualitative analysis of biofilm changes. Detection of biofilm growth and treatment within the platform, as shown in figure 1, is achieved via the *in situ* measurement of biofilm optical density (OD) [33, 39–41], where the use of linearly arrayed photopixels enables the monitoring of biofilm OD at various points over the length of the microchannel. OD values provide a metric for an amount of light transmitted through a biofilm relative to an amount of light incident on the biofilm, and therefore provide a measure of biofilm absorption. Since biofilm absorption increases with biofilm mass, OD values correlating to biofilm mass provide a non-invasive approximation of the growth stage of biofilms [33, 39–41]. Therefore, real-time monitoring of OD values via the arrayed photopixels of the Micro-BOAT platform can illustrate the matureness of biofilms at various points within the microchannel, thereby enhancing biofilm characterization capabilities.

The non-invasive, label-free, continuous monitoring capabilities of OD measurement enables the Micro-BOAT platform as an adaptive research tool that can find use in new treatment discovery applications such as the BE presented here and other investigations of microbial mechanisms.

Leveraging the small scale of the Micro-BOAT setup, the voltage potential required to induce the appropriate intensity of electric field in the platform (0.25 V) was further reduced below the electrolysis potential of the media [27, 33] compared to the conventional cuvette system [29]. Planar, thin-film electrodes integrated with the microfluidic channels of the Micro-BOAT platform were utilized to induce electric fields within the microfluidic growth reactors (figure 1(b)). Studies conducted using the Micro-BOAT platform indicate that when the bioelectric effect is applied to *E. coli* BL21 pGFP biofilms matured within the microfluidic reactors of the Micro-BOAT platform in the presence of antibiotics (10 μg ml^{-1} of gentamicin), significant decreases in both total biomass and viable cell density are observed in comparison to the traditional antibiotic therapy using only gentamicin. The dimensions of the electrodes in comparison to the height of the microfluidic growth reactors (0.2 μm electrode thickness versus 100 μm channel height) demonstrate the efficacy of the BE induced via sub-micron thick thin-film electrodes. Furthermore, the

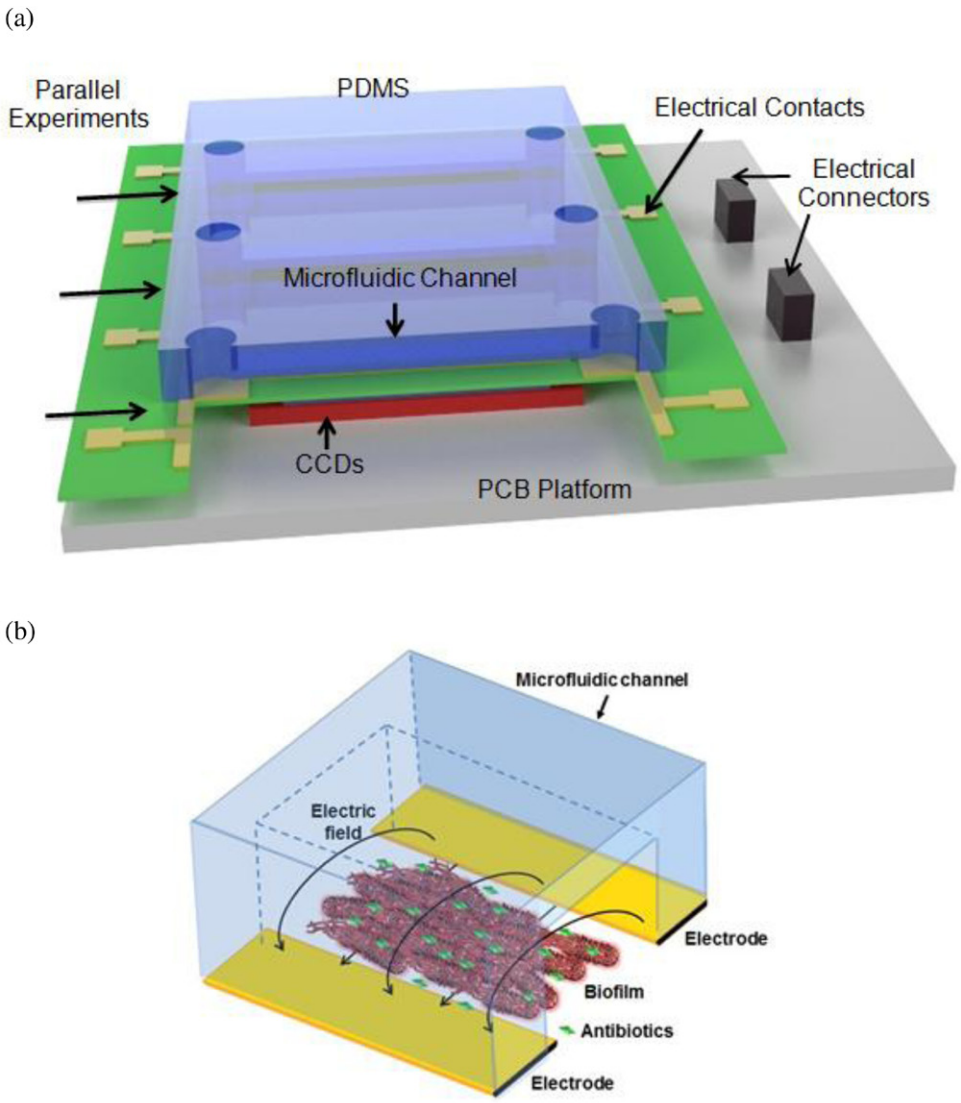

Figure 1. (a) Schematic of the microfluidic biofilm observation, analysis and treatment (Micro-BOAT) platform used for the demonstration of the bioelectric effect (BE). The platform is capable of performing six experiments in parallel on a single chip. Real-time biofilm monitoring is achieved via the measurement of biofilm OD using charge-coupled devices (CCD) and a tuned light emitting diode (LED) source (not shown). Based on the resolution of the CCD, which allows for biofilm OD monitoring along the length of an entire microfluidic channel, both averaged and localized biofilm OD values are obtained. The BE can be applied to selected channels on the Micro-BOAT platform through electrical contacts fabricated on the micro-channel substrate. (b) Close-up schematic of the BE biofilm treatment in a single microchannel, which uses planar electrodes, exposed on each side of the microchannel, to emit an electric field comprising a 10 MHz AC signal at 1.25 V cm^{-1} (corresponding to 0.25 V for 2 mm electrode spacing)with a 1.25 V cm^{-1} DC offset.

Micro-BOAT system provides an instrument for the study of biofilm treatments in micro-scale environments, where validation of the BE using biocompatible parameters represents a significant step forwarding biofilm infection treatment.

2. Methods

2.1. Micro-BOAT platform design and fabrication

The Micro-BOAT tool is an integrated microsystem consisting of an electronics platform with linear array charge-coupled devices (CCD) and supporting electrical components, a micro-fabricated patterned base, and molded microfluidics. CCDs (TSL202R, Texas Advanced Optoelectronic Solutions) used for optical density (OD) detection are integrated on a custom printed circuit board (PCB, Advanced Circuits) to enable six parallel experiments on a single chip measuring 9.5 cm × 8.1 cm. The CCDs feature 128 × 1 linear photopixel arrays.

A 500 μm thick Pyrex^{TM} wafer serves as a transparent substrate for the patterned base. Gold electrodes patterned on the substrate provide electric fields required to induce the BE, while simultaneously limiting peripheral light from entering the CCD components. The electrodes (Cr/Au 15 nm/200 nm), fabricated by physical vapor deposition on top of photoresist (AZ-5214, MicroChemicals GmbH) followed by liftoff, feature 2 mm spacing within the microchannels.

Molded microfluidic structures are fabricated through a standard polydimethylsiloxane (PDMS) process [34].

Reversible bonding of the PDMS channel to the patterned substrate is achieved by applying methanol to the PDMS, then aligning and placing it onto the Pyrex™ chip. The resulting microfluidic chambers measure 100 μm deep, 2.5 mm wide, and 1.75 cm long for a total chamber volume of 4.375 μl. The microfluidic chamber is connected to an external syringe pump (Cole Parmer 74900), operating in withdrawal mode to minimize device leakage.

Actuation of the CCDs in the Micro-BOAT platform requires a power source, drive clock, and serial input bit provided by an external power supply (Agilent E3631A) and accompanying function generators (BK Precision 4040). Signal readout from the CCDs is achieved using a data acquisition device (NI USB-6221, National Instruments). All external electrical signals are integrated with the Micro-BOAT platform via wire-to-board connectors (Molex Connector Corporation) and BNC cables (L-Com Global Connectivity). Illumination of the Micro-BOAT system for OD measurement is achieved using a diffusive edge-lit LED light panel to provide uniform illumination of the system (Luminous Film USA). Light emission is tuned to a wavelength spectrum centered at 630 nm by a polycarbonate lighting gel film (Roscolux #120, Rosco Laboratories) in order to match the peak sensitivity of the CCD components. The entire assembly is placed within an incubator (I5110, Labnet International, Inc.) at 37 °C.

2.2. Micro-BOAT characterization experiments

To confirm linearity of the CCD sensing platform, suspensions of *E.coli* BL21 pGFP were cultured and diluted to produce a range of known optical density samples. *E. coli* samples are prepared by first growing a bacterial culture in Lysogeny Broth (LB) media for 24 h at 37 °C in a sample shaker at 250 rpm. The density of this sample is then tested using a spectrophotometer (Beckman Coulter, Inc.) to establish the OD_{600} of the culture, diluted in LB media, and re-tested. For the results presented here, the prepared suspensions featured OD_{600} values of 0.15, 0.29, 0.59, 1.17, 2.34 and 4.68 [AU] (figure 2). Bacterial suspensions are inoculated in the microfluidic channel of the Micro-BOAT platform for a brief period and 25 unique OD measurements recorded for each sample using NI LabVIEW (LabView 2010 SP1, National Instruments). Deionized (DI) water is used to flush the channel of bacterial cells between each sample. Changes in OD measured by the Micro-BOAT system are calculated using the following equation for all samples, which is based on that used for typical absorbance measurements [42],

$$\text{Absorbance [AU]} = -\log_{10}(I/I_o),$$

where I is the intensity of the transmitted light, and I_o is the initial incident intensity. Due to a linear relationship between photopixel irradiance and pixel output voltage, the equation for optical density follows directly from that above,

$$\text{Optical Density [AU]} = -\log_{10}(V/V_o),$$

where V is the average voltage output of the 128 photopixels for each OD measurement, and V_o is the average output voltage of these pixels when the channel is filled solely with LB growth media. Device sensitivity is calculated by the ratio of optical sensor noise, given as 1.0 mV, to sensor sensitivity, which was determined to be 10.50 mV/AU from the slope of the linear fit in figure 2.

Capabilities to detect spatiotemporal changes in optical density within the Micro-BOAT system are determined by flowing optically dense droplets ($OD_{600} \approx 45$) in a translucent liquid and demonstrating droplet detection using the platform. DI water prepared in a 10 : 1 ratio with propylene glycol dye (McCormick & Company, Inc.) creates a homogeneous solution. Droplets are inserted in a flow stream of translucent mineral oil by puncturing the Tygon tubing used for sample flow with a 27-gauge, 0.5 inch needle (Becton, Dickinson and Company). The flow of oil with separated, water-based droplets is provided at a volumetric flow rate of 0.25 ml h^{-1} and detected using the Micro-BOAT as described previously.

2.3. Bacterial strains and experimental procedure

E. coli BL21 is frequently used in clinically relevant bacterial investigations, as it is a well-studied biological system and is well-suited for protein over-expression [38]. In this study, *E. coli* BL21 modified with a plasmid for expression of green fluorescent protein (pGFP) is used for biofilm studies to enable endpoint fluorescence microscopy in which metabolically active bacteria fluoresce green. For the treatment experiments presented in this work, bacterial cultures are initially grown in LB growth media to an $OD_{600} \approx 0.25$.

Testing is performed by initially disinfecting the microfluidic channels of the Micro-BOAT platform using 70% ethyl alcohol under flow. After rinsing with DI water, bacterial suspensions, prepared as above, are inoculated without flow for 2 h to allow for bacterial attachment to the substrate [35]. LB media is then continuously supplied to the channel for 24 h at 20 μl h^{-1} (average flow velocity of 30 μm s^{-1} for the given channel dimensions) to replenish nutrients and foster biofilm growth. Treatments are started after 24 h of growth and continued for an additional 24 h. Antibiotic treatments utilize gentamicin (Invitrogen Inc.) at a 10 μg ml^{-1} concentration in LB media [28, 29]. To achieve an exchange of fluid sources during experiments with minimal impact, flow is stopped and the inlet tubing transferred to the new source before reinitializing flow. OD measurements are taken non-invasively in real-time for both average and localized changes in OD. Initial optical density of the biofilm is measured 30 min after the preliminary inoculation period and the start of LB media flow. Measurements are obtained every 8 min thereafter and recorded using LabVIEW.

Four treatment conditions were applied to biofilms (i.e. control, only antibiotic treatment, only electric field, and BE), with each treatment condition being performed three times to demonstrate the reported standard deviations. The Micro-BOAT platform includes six parallel microfluidic channels (figure 1), with each experiment utilizing two microfluidic channels for each of three different treatment conditions. For each experiment, the same Pyrex substrate was used, and the PDMS replaced with new PDMS made using the same mold.

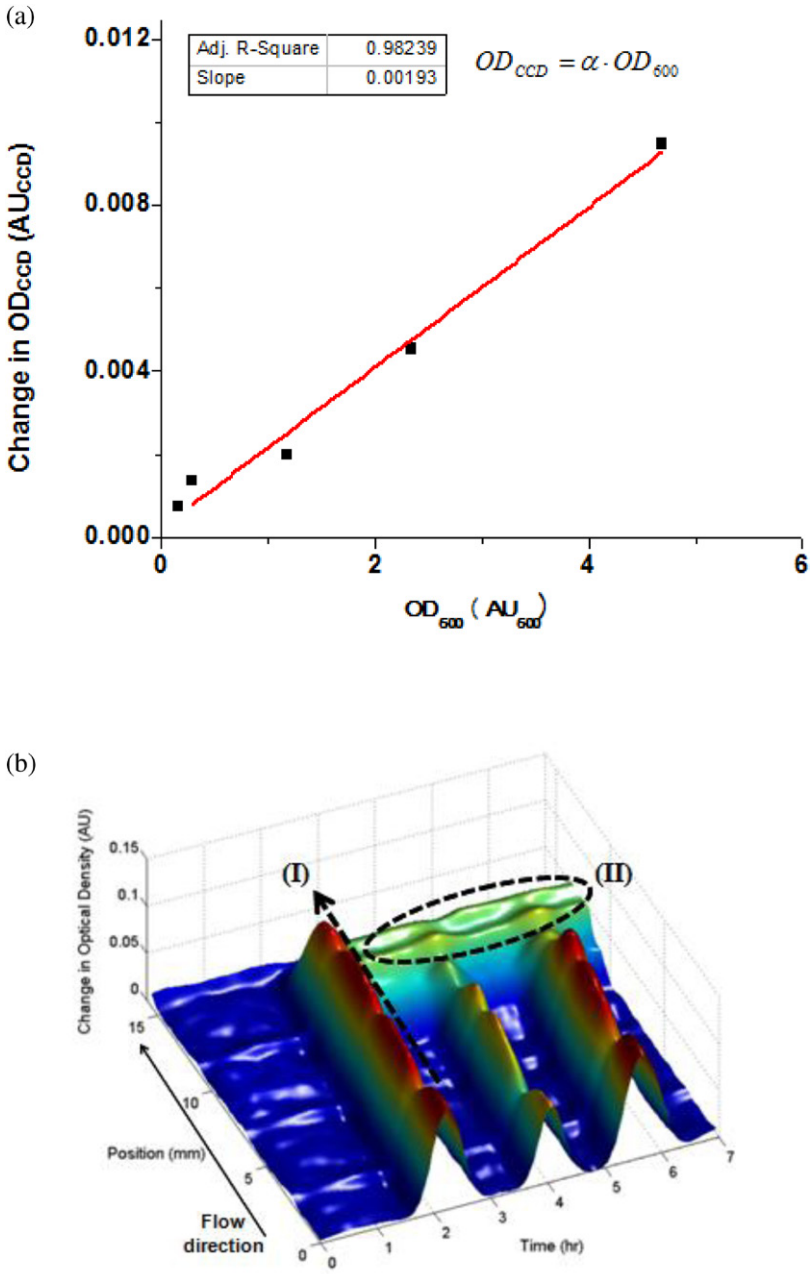

Figure 2. (a) Optical densities (OD_{CCD}) measured using the Micro-BOAT platform for bacterial suspensions of established OD_{600}. The results demonstrate a linear relationship that verifies the correlation of OD_{600} to OD_{CCD} measured on-chip using the Micro-BOAT system. Based on a linear conversion using the slope (α) of the linear fit, the optical density measurement of the platform (OD_{CCD}) shows a detection limit of approximately 0.002 AU_{CCD} corresponding to ~0.095 AU_{600}. (b) Demonstration of spatiotemporal OD monitoring in the Micro-BOAT platform. Optically dense water droplets with a measured OD_{600} of approximately 45AU_{600} are separated in a flow of transparent mineral oil and supplied to a single channel of the Micro-BOAT platform to demonstrate real-time OD monitoring. The arrow indicates the flow direction from inlet to outlet of the microfluidic channel. Here, the passage of three droplets is detected within the microfluidic channel (first droplet highlighted as (I)), where a portion of the first droplet adheres to the surface of the microfluidic channel resulting in a stationary area of increased OD within the microchannel (II).

Treatment efficacy was measured by recording changes in biofilm OD during the treatment relative to an initial biofilm OD measured after a 24 h maturation period.

2.4. Bioelectric effect

The intensity and frequency of the electric field for the BE has been characterized previously with a traditional macro-scale cuvette setup focused on preventing electrolysis of biological media (at around 0.82 V) [27–29]. The electric field utilized both AC and DC signals simultaneously (superimposed(SP) field) [29]. The frequency (10 MHz) of the AC signal was chosen based on reports from literature [19, 25, 26]. Due to the implementation of the BE in the Micro-BOAT platform, the required electric voltage to induce the electric field (1.25 V cm^{-1}) was reduced to 0.25 V for 2 mm separated electrodes, safely

below the electrolysis potential (~ 0.82 V). The reduced potential of 0.25 V was used for both the AC and DC signal amplitudes. The concentration of antibiotic (10 μg ml^{-1} of gentamicin) was selected based on previous work [33]. Hence, the BE verified in this work is a combination of the SP field (1.25 V cm^{-1} magnitude of sinusoidal 10 MHz and 1.25 V cm^{-1} DC offset) with the antibiotic gentamicin (10 μg ml^{-1}).

2.5. Microscopy and image analysis

At the conclusion of bacterial treatment experiments, live/dead cell staining and microscopy are performed. Performing live/dead cell staining and microscopy at the end of biofilm treatment allows for the analysis of surface-adhered biofilms. It is understood that during biofilm development, parts of surface-adhered biofilm may detach and move to other surfaces, resulting in the spreading of biofilms [4–6]. However, even considering this nature of biofilm growth, quantification of surface-adhered biofilm cell densities after different treatments can provide comparable data for evaluating biofilm treatment efficacy [41, 46, 47]. This work therefore concentrates on the investigation of live and dead cell densities of surface-adhered biofilms within a microchannel.

To execute adhered cell staining, the microfluidic channel is first rinsed with phosphate buffer saline (PBS) at a rate of 200 μl h^{-1} for 1 h to remove non-adherent bacterial cells. The remaining biofilm is then treated using a red propidium iodide stain (Invitrogen no L7012) to allow imaging of unviable bacteria in the biofilm. The stain is provided in a 1.5 μl 1 ml^{-1} PBS concentration at a rate of 200 μl h^{-1} for 2 h to ensure complete staining of non-living cells, while the live cells are naturally fluorescent due to the expression of GFP. Subsequently, the channel is rinsed using PBS at 200 μl h^{-1} for 1 h to remove unabsorbed propidium iodide, thereby increasing the contrast of biofilm imaging.

Microscopy is performed using a fluorescent microscope (Olympus BX60) at 20 × magnification to observe individual bacteria. Both total fluorescence and green fluorescence mode images are obtained from multiple locations of each sample (total number of images per treatment, $N = 7$). Quantitative analysis of the images is performed using the image-processing software ImageJ (ImageJ 1.44, USA). The percentage of viable biofilm bacteria surface coverage with respect to total biofilm surface coverage is obtained by first filtering red and blue colors from the fluorescence images, creating a binary image conversion with respect to the background color of each image, and finally calculating the non-background surface coverage. The percentage of viable bacteria is calculated as the ratio of green fluorescent surface coverage to total fluorescent surface coverage for each image sample.

Analysis of OD data is performed using NI LabVIEW and MATLAB. Average OD measurements utilize the mean voltage output value from the 128 CCD photopixels at each measurement period. Analysis of spatiotemporal changes in OD is performed using MATLAB.

3. Results

3.1. Micro-BOAT platform characterization

Prior to utilizing the microfluidic platform to investigate the efficacy of the BE in reducing established bacterial biofilms, characterization of the microsystem is performed to determine the sensitivity of the measurement technique and to validate spatiotemporal detection capabilities. Two specific studies are conducted: (1) device sensitivity is characterized by comparing changes in OD measured using the Micro-BOAT platform to known OD values at 600 nm (OD_{600}), and (2) spatiotemporal detection capabilities of the Micro-BOAT platform are validated by measuring real-time changes in OD along the microfluidic channel.

The response of the Micro-BOAT platform to known changes in OD_{600} is presented in figure 2(a). The results demonstrate a linear response between OD_{600}measured bya spectrophotometer and changes in OD as measured by the Micro-BOAT system (OD_{CCD}). The observed linear response is anticipated due to the irradiance response of the CCD photopixels used in the Micro-BOAT system. Due to the difference in OD measurement techniques utilized by the spectrophotometer and Micro-BOAT platforms, the OD measurement units are correlated using the slope of the linear fit (α ~ 0.002) to convert from OD_{600} [AU_{600}] to OD_{CCD} [AU_{CCD}]. A consistent OD_{600} biofilm detection limit of 0.095AU_{600} was calculated for a full range of optical densities relevant for biofilm growth experiments [39–41] . The observed relationship enables the approximation of biofilm OD at 600 nm, a standard in clinical fields, using the Micro-BOAT platform.

Additionally, as bacterial biofilms are stochastic biological organisms demonstrating spatial variation and colony expansion through sloughing and reattachment [4–6, 33], the spatiotemporal tracking capabilities of the Micro-BOAT system were investigated to determine the utility of the Micro-BOAT system for investigating the variable growth characteristics of bacterial biofilms. The capability of the micro-BOAT platform to monitor spatiotemporal changes in biofilm OD is evaluated by studies in which optically dense droplets ($OD_{600} \approx 45AU_{600}$) are supplied under flow and detected in real-time. Localized OD detection is demonstrated and presented in figure 2(b). Passage of three exemplary droplets is detected within the microfluidic channel (first droplet highlighted as (I) in figure 2(b)). A portion of the first droplet adheres to the surface of the microfluidic channel, resulting in a stationary area of increased OD within the microchannel ((II) in figure 2(b)). The measured flow velocity of droplets within the microchannel concurs with theoretical calculations given the channel geometry and volumetric flow rate implemented for the experiment, thereby validating the platform for the monitoring of localized changes in biofilm OD.

Cumulatively, characterization of the Micro-BOAT device confirms its functionality as a platform for continuous, label-free, non-invasive OD monitoring of both average and spatiotemporal changes in bacterial biofilm OD.

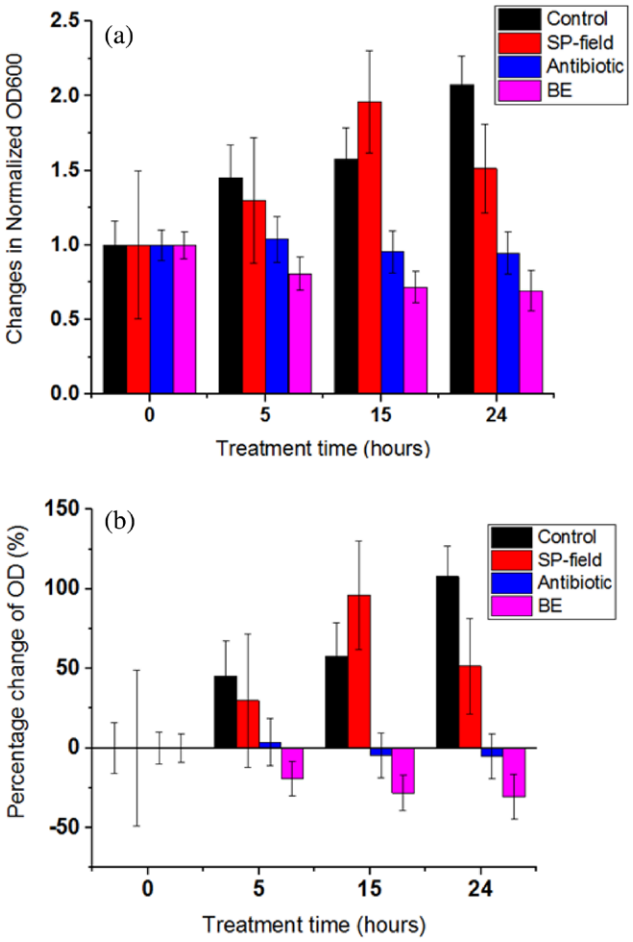

Figure 3. (a) Changes in normalized OD_{600} values are presented for each of four treatment methods. The changes are shown with respect to initial OD_{600} values that are recorded after the 24 h maturation period. In the figure, $T = 0$ h corresponds to the end of the 24 h maturation period, and the beginning of treatment. Both the control and SP biofilms display increases in biomass, evidenced by increases in optical density, while the biofilms treated by antibiotics independent of an SP field and the BE treated biofilms showed decreases in optical density over the course of treatment. Each bar represents an average change in OD_{600} for three independent experiments at representative time points, with standard deviations also shown for the three independent experiments ($N = 3$ for each treatment). Changes in OD_{600} are statistically significant (ANOVA, $P < 0.001$) between the treatments. The four treatments were applied to *E. coli* BL21 pGFP biofilms following a 24 h maturation period in an incubator maintained at 37 °C. Biofilms undergoing controlled growth (no electric field or antibiotic treatment) and those treated solely with an electric field display overall increases in bacterial biomass. Traditional antibiotic therapy and BE treatments demonstrate significant decreases in bacterial biomass (5% and 31%, respectively). At the conclusion of the 24 h treatment period, average OD_{600} values for the BE and antibiotic treated biofilms are compared, with the BE treated biofilms demonstrating a 26% increase in biomass inhibition compared to traditional treatment using antibiotics independent of an externally applied electric field. (b) Percentage changes in *E. coli* BL21 pGFP biofilm OD_{600} during the 24 h treatment cycle demonstrated in figure 3(a). The absolute changes in OD_{600} observed in figure 3(a) are computed as percentage changes in biofilm OD_{600} relative to the initial OD of the biofilms at the end of the 24 h maturation period, as shown in table 1. Error bars indicate the standard deviations between the three independent experiments of each treatment ($N = 3$ for each treatment).

Table 1. Absolute changes in biofilm OD_{600} and corresponding percentage changes in OD_{600} measured relative to initial OD_{600} values are shown for biofilms undergoing four different treatment conditions at representative points in time during the treatment phase. The OD conversion from CCD to OD600 was based on the linearity between them as shown in figure 2. Initial OD_{600} values represent total biofilm biomass after a 24 h maturation period.

	Time	Initial	5 h	15 h	24 h
Control	Average OD_{CCD}	0.007	0.010	0.011	0.015
	Average OD_{600}	3.50	5.08	5.52	7.27
	Normalized OD_{600}	1.00	1.45	1.58	2.08
	Percentage change	0%	45.1%	57.8%	107.7%
SP field	Average OD_{CCD}	0.008	0.010	0.015	0.012
	Average OD_{600}	3.83	4.98	7.51	5.80
	Normalized OD_{600}	1.00	1.30	1.96	1.52
	Percentage change	0%	29.9%	96.0%	51.5%
Antibiotic	Average OD_{CCD}	0.021	0.021	0.020	0.019
	Average OD_{600}	10.27	10.66	9.79	9.72
	Normalized OD_{600}	1.00	1.04	0.95	0.95
	Percentage change	0%	3.8%	−4.6%	−5.3%
BE	Average OD_{CCD}	0.024	0.020	0.017	0.017
	Average OD_{600}	12.10	9.78	8.69	8.41
	Normalized OD_{600}	1.00	0.81	0.72	0.69
	Percentage change	0%	−19.2%	−28.2%	−30.5%

3.2. Micro-scale BE for enhanced biofilm treatment

3.2.1. Change of biomass by the BE. The measurement of biomass variation via changes in biofilm OD is a critical indicator of the efficacy of new antimicrobial treatments [19–21, 28, 39–41]. Here, total biomass changes under different treatments are continuously monitored via real-time OD measurement using the Micro-BOAT platform. Model *E.coli* BL21 pGFP biofilms are matured in four different microfluidic growth reactors at 37 °C and subsequently treated. Four methods are tested, one in each microfluidic channel, in order to determine the relative efficacy of each: (1) negative control, without an applied electric field or antibiotic treatment, (2) treatment utilizing an SP electric field in the absence of antibiotics, (3) treatment utilizing antibiotics in the absence of an electric field (10 μg ml^{-1} of gentamicin), and (4) the BE, applied by combining the SP field with the same antibiotic treatment as in (3). After a 24 h maturation period, the initial biofilm OD_{600} in each trial was determined, as well as the average OD_{600} of the initial biofilms

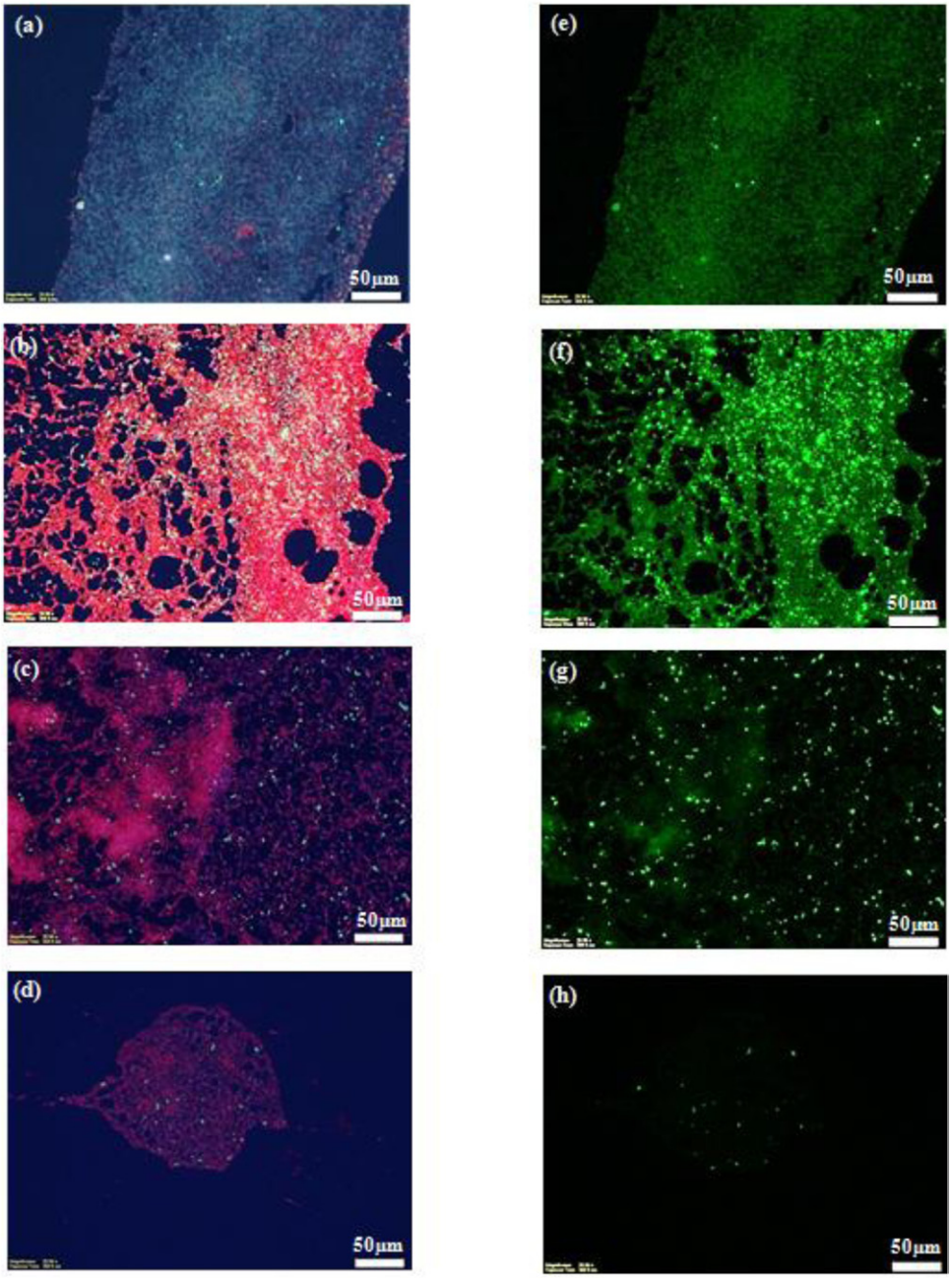

Figure 4. Representative fluorescence microscopy images of biofilms in the Micro-BOAT channels following maturation and treatment. The total biomass fluorescence images (left column) and viable biomass fluorescence (right column) of biofilms show control ((a) and (e)), SP electric field ((b) and (f)), traditional antibiotic ((c) and (g)), and BE ((d) and (h)) treated biofilms. Biofilms treated with the BE showed reduced biomass (d) as well as low viable bacterial cell density (h). Seven fluorescence images were taken for each of the four treatment methods ($N = 7$), with the images presented here representing regions of high biofilm density.

(7.42, $N = 12$) and the standard deviation of initial biofilm OD_{600} (4.41, $N = 12$). The trials demonstrate a 59% total biomass variation in initial biofilm OD_{600} between the microfluidic channels. Such variation can be attributed to the variant spatial biofilm growth in the separated microfluidic channels that can result from differences in nutrient concentration along the microchannels and shear stresses induced by biofilm growth within the microchannels [41, 46, 47] . Treatment efficacy evaluation is therefore focused on percentage changes in biofilm mass attributable to each of the different treatment methods.

Figure 3(a) demonstrates the changes in normalized OD_{600} within each microchannel of the Micro-BOAT system relative to the initial OD_{600} of the biofilm in that channel. Figure 3(b) presents the same data as percentage changes in biofilm OD. Percentage changes in biofilm OD_{600} were calculated using the equation shown below.

$$\text{Percentage changes in } OD_{600} = \frac{(\text{Selected Time } OD_{600} - \text{Initial } OD_{600})}{\text{Initial } OD_{600}} \times 100$$

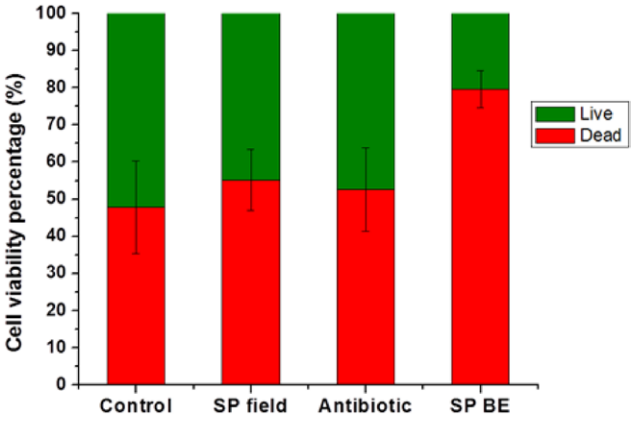

Figure 5. The percentage of viable biofilm bacteria with respect to total biomass after each treatment is calculated using image processing software (ImageJ 1.44). The results include the average of seven image analyses ($N = 7$) for each of the four treatment methods.Viable cell percentages and standard deviations are obtained with respect to total fluorescent mass surface coverage using a binary image conversion (see section 2). The relative density of non-viable cells in biofilms treated by the BE is shown to increase 56% in comparison to treatments using antibiotics independently ($p = 0.019$).

OD measurements are recorded *in situ* and averaged along the entire microfluidic channel. Table 1 additionally includes the measured OD values for each biofilm at the relevant time points shown in figure 3(a). Following the treatment phase, biofilms undergoing controlled growth (control) and exposure to the SP electric field treatments demonstrate increases in biofilm OD_{600} of approximately 108% and 52%, respectively, corresponding to increases in bacterial biomass and overall biofilm growth [39–41] . Here, increases in biofilm mass over the course of the treatment phase of the experiments are attributed to the continued development, growth, and spread of the biofilm, enabled by the continuous supply of fresh nutrients to the microchannels during the 24 h treatment period. Standard antibiotic treatments (gentamicin) demonstrate an average net decrease in biofilm OD_{600} of 5% over the course of treatment. By final comparison, biofilms treated using the BE display average net decreases in OD of 31%, a 26% decrease in total biomass compared to treatment by antibiotics alone. This drastic improvement in treatment efficacy was achieved without an increase in antibiotic concentration and while only applying a low intensity electric field. Thus, the enhanced biocidal effects demonstrated by the BE represent a significant advantage of this method over treatments relying exclusively on antibiotics.

3.2.2. Viable cell reduction by the BE. In addition to the quantification of changes in bacterial biomass via an OD method in the Micro-BOAT platform, each treatment is evaluated for biocidal efficacy using dead cell staining and fluorescence microscopy for further verification of the treatment efficacy of the BE. To perform biofilm imaging, unviable cells in the *E. coli* BL21 pGFP biofilms are stained red, while metabolically active bacteria appear green based on the expression of GFP. Figure 4 presents representative total fluorescence (left column, figures 4(a)–(d)) and green fluorescence images (right column, figures 4(e)–(h)) for each of the four treatments. The total fluorescence images reveal both viable and unviable bacteria in the biofilm, corresponding to overall biomass in the microfluidic channel following treatment. As shown in figure 4(d), biofilms treated with the BE show the least amount of bacterial biomass, indicating enhanced biomass reduction compared to biofilms treated solely with antibiotics (figure 4(c)). Additionally, biofilms treated with the BE demonstrate a lower density of live cells (figure 4(h)) compared to the other treatments, as shown in the green fluorescence images. The microscopy images (figures 4(d) and (h)) illustrate a strong reduction in both overall bacterial biomass and viable bacteria within biofilms treated by the BE.

A quantitative analysis of viable biofilm bacteria is performed, in which the percentage of metabolically active bacteria in each sample is calculated based on the surface coverage of live bacteria (green fluorescence images) with respect to the total fluorescent biomass (see section 2) [43]. The result in figure 5 represents the percentage of viable bacteria (green fluorescent mass) within a given biofilm mass (total fluorescent mass). As shown in figure 5, the BE treatment results in 56% lower relative viable cell density compared to biofilms treated exclusively with antibiotics, further demonstrating the improved treatment efficacy of the BE in comparison to traditional treatments and reinforcing the OD measurements presented previously (figure 3).

4. Discussion

Improved bacterial biofilm treatment efficacy has been demonstrated at the micro-scale by combining externally applied electric fields with traditional antibiotic treatments to induce the BE. Using the developed Micro-BOAT platform featuring planar thin-film electrodes integrated with microfluidic growth chambers, an electric field characterized to be well within biocompatible limits was combined with low concentrations of the antibiotic gentamicin to yield repeatable results showing significant biofilm reduction. With respect to treatments implementing identical concentrations of antibiotics only, this was quantified as a 26% further decrease in total biomass (figure 3 and table 1) accompanied by a 56% reduction in relative viable bacteria density (figure 5). This enhanced biofilm treatment efficacy is attributed to the simultaneous application of an electric field with the antibiotic gentamicin. In comparison to our previous macro-scale BE demonstration [28, 29], the effective biofilm reduction (~400 times more viable cell reduction than only antibiotic therapy) was decreased in this work, likely since the electric field through the microfluidic channel was not uniform. This was due to the planar electrode structure as opposed to the side-walled electrodes in the traditional cuvette setup. Nevertheless, the first on-chip demonstration of the BE within the Micro-BOAT platform using low intensity electric fields within biocompatible limits [27] encourages the prospective use of this technique for varied applications in the future, including localized *in vivo* and *in vitro* biofilm treatments such as those targeting infected prosthetics and biofilms in catheters.

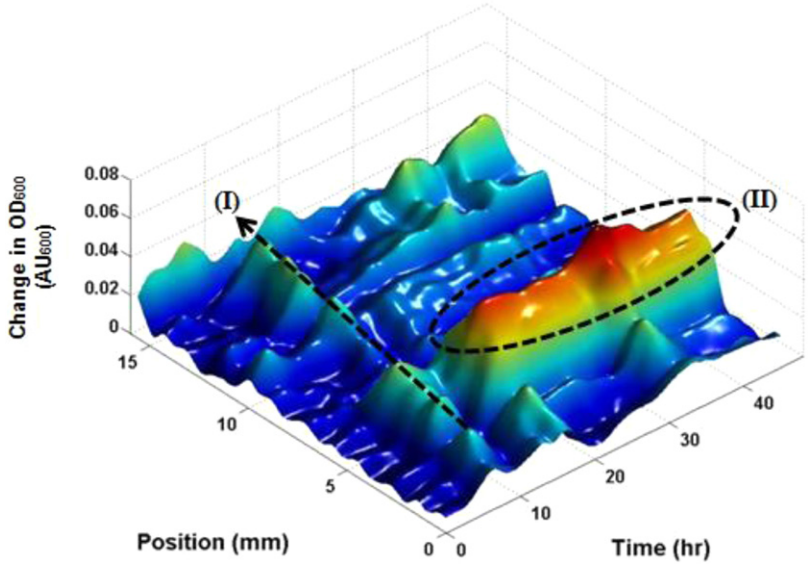

Figure 6. Surface reconstruction illustrating a representative morphology of an *E. coli* BL21 pGFP biofilmgrowing within a microchannel of the Micro-BOAT platform. The biofilm shown here was matured under constant flow rate for 48 h at 37 °C within the Micro-BOAT platform and demonstrates typical biofilm morphology and density. (I) can be indicative of biofilm detachment and propagation along the microfluidic channel due to shear flow forces. (II) is indicative of permanent biofilm attachment to the substrate and the localized development of bacterial biofilm within the microchannel. Other spatiotemporal changes in OD observed over the 48 h period are attributable to spatiotemporal biofilm development within the microfluidic environment.

To evaluate the biocidal effects of the various treatments, the surface coverage of live cells within biofilms (figure 4, right column) was determined with respect to total bacterial biomass (figure 4, left column). This quantification approach relies on a 2D surface projection of a biofilm as imaged by fluorescence microscopy. Although biofilms are considered 3D structures, a 2D projection of biofilms contains critical information for the approximation and analysis of biofilm characteristics, including biofilm structure, density, and surface coverage [44]. In this study, the 2D surface projection method was used to quantify viable biofilm cell density, revealing a statistically significant difference in viable cell density for biofilms treated using the BE in comparison to other treatments ($p < 0.05$, figure 5). Such results further affirm the enhanced biocidal effects of the BE observed via OD monitoring by the Micro-BOAT platform.

Validation of the BE using thin-film planar electrodes in a micro-scale environment represents a critical step in the development of BE treatments for future clinical applications. The reported levels of efficacy are statistically significant and support the use of thin-film planar electrodes to induce the BE, with the current Micro-BOAT platform demonstrating efficient treatment in a microfluidic channel that is 500 times deeper than the thickness of the electrodes (0.2 μm thin-film gold electrodes in a 100 μm deep channel). The use of thin-film electrodes to induce electric fields enables scaling of treatment systems utilizing the BE to sub-micron thicknesses while maintaining broad effective treatment areas. Such a method provides a potential approach for localized infection treatments that requires reduced antibiotic dosages compared to current therapies.

The Micro-BOAT platform presented herein has clear value as a research tool for scientific studies in microbiology and drug research, by leveraging the unique advantages of the developed system. The integration of linear array CCD components provides insight into both average and localized changes in biofilm density within the microfluidic channel that is achieved through OD monitoring.

We have also demonstrated that the Micro-BOAT system is effective for spatiotemporal monitoring of significant change in OD (e.g. $OD_{600} \approx 45$, figure 2(b)). Additionally, a representative spatiotemporal biofilm monitoring result was obtained that displays physical changes in microbial structure and density, including detachment ((I) in figure 6), localized growth ((II) in figure 6), and the aggregation of free-flowing particulates over an established biofilm structure, that are uniquely detectable using the Micro-BOAT platform. With respect to existing methods used for the imaging of biofilm structure and morphology, including confocal and fluorescence microscopy, the developed platform represents a viable alternative for conducting biofilm imaging with sufficient resolution and detection limits to conduct biofilm investigations without incurring the expense or bulk inherent to these systems.

Furthermore, the high throughput capabilities of the Micro-BOAT platform, which also leverages controlled sample flows, small sample volumes, and increased environmental control [34–38], can aid other fields of microbiology in which experiments featuring controlled growth environments and/or time-consuming experimental repetition are the standard [6, 33, 45]. As demonstrated, the platform enables the correlation of OD measurements obtained via the Micro-BOAT platform to other common methods, including optical absorbance at 600 nm, with limited calibration. In contrast to traditional detection methods, such as confocal microscopy, fluorescence microscopy, or bacterial colony counting,

which are typically limited to end-point evaluations of biofilm structure and density, the Micro-BOAT platform enables the monitoring of both overall and spatial changes in biofilm density in real-time. The non-specific detection achieved with broad spectrum OD measurement and analysis (wavelengths 550 to 700 nm) makes this an ideal platform for biofilm studies pertaining to various clinically relevant bacterial strains without the need for specialized labeling, a principal benefit of this method. Future generations of the Micro-BOAT device may utilize a tunable optical source to enable potential fluorescence imaging within the same system. Based on the unique real-time, high throughput, and broad spectrum OD measurement capabilities of the Micro-BOAT platform, we expect the system to be applied for continued research efforts in the future, including those aimed at microbiological studies and the development of other novel biofilm treatment methods.

5. Conclusion

This work demonstrates significant enhancements in biofilm treatment utilizing the BE in a micro-scale system. A Micro-BOAT platform used to demonstrate the BE on-chip provides not only real-time monitoring of biofilm OD *in situ*, but additionally can achieve spatiotemporal tracking of changes in bacterial biomass via OD measurement. The BE presented in this work demonstrates drastically improved biofilm treatment efficacy, showing reductions in both total biomass and viable bacterial density, in a biofilm growth reactor of considerably greater depth than the thickness of the electrode structures used to induce the electric fields. Demonstration of the BE in the Micro-BOAT platform verifies both the integration capabilities of this method with microsystems, as well as the scale-down of the treatment method for clinical applications. Validation of this method using planar thin-film electrodes and low intensity electric field potentials has far-reaching implications by enabling its use for potential patient care applications. Specifically, we believe demonstration of the BE in the microsystem presented herein directs further device development for *in vivo* and *in vitro* biofilm infection treatment, while additionally providing a new research tool for scientific studies, including those aimed at drug discovery and antimicrobial mechanism investigations.

Acknowledgments

The authors would like to acknowledge the Robert W. Deutsch Foundation and the National Science Foundation (CBET #1160005, CBET #1264509, EFRI #0735987) for financial support. The authors also would like to thank the Maryland Nanocenter and its Fablab for cleanroom facility support.

Author contributions

Y W Kim and M P Mosteller have contributed equally to this work.

References

[1] Ehrlich G D, Hu F Z, Lin Q, Costerton J W and Post J C 2004 Intelligent implants to battle biofilms *ASM News* **70** 127–33
[2] Darouiche R O 2004 Treatment of infections associated with surgical implants *New England J. Med.* **350** 1422–9
[3] Khoury A E, Lam K, Ellis B and Costerton J W 1992 Prevention and control of bacterial infections associated with medical devices *ASAIO J.* **38** 174–8
[4] Costerton J W, Stewart P S and Greenberg E P 1999 Bacterial biofilms: a common cause of persistent infections *Science* **284** 1318–22
[5] Ghannoum M and O'Toole G A 2004 *Microbial Biofilms* (Washington, DC: ASM Press)
[6] Stoodley P, Sauer K, Davies D and Costerton J W 2002 Biofilms as complex differentiated communities *Annu. Rev. Microbiol.* **56** 187–209
[7] Fux C A, Stoodley P, Hall-Stoodley L and Costerton J W 2003 Bacterial biofilms: a diagnostic and therapeutic challenge *Expert Rev. Anti-Infective Ther.* **1** 667–83
[8] Characklis W 1981 Bioengineering report: Fouling biofilm development: a process analysis *Biotechnol. Bioeng.* **23** 1923–60
[9] Potera C 1999 Forging a link between biofilms and disease *Science* **283** 1837–9
[10] Hall-Stoodley L, Costerton J W and Stoodley P 2004 Bacterial biofilms: from the natural environment to infectious diseases *Nat. Rev. Microbiol.* **2** 95–108
[11] Costerton W, Veeh R, Shirtliff M, Pasmore M, Post C and Ehrlich G The application of biofilm science to the study and control of chronic bacterial infections *J. Clin. Invest.* **112** 1466–77
[12] Del Pozo J and Patel R 2007 The challenge of treating biofilm-associated bacterial infections *Clin. Pharmacol. Therapeutics* **82** 204–9
[13] Donlan R M 2001 Biofilms and device-associated infections *Emerg. Infect. Dis.* **7** 277–81
[14] Zimmerli W 2006 Prosthetic-joint-associated infections *Best Pract. Res. Clin. Rheumatol.* **20** 1045–63
[15] Stewart P S 2002 Mechanisms of antibiotic resistance in bacterial biofilms *Int. J. Med. Microbiol.* **292** 107–13
[16] Sutherland I W and Suthe I 1977 *Surface Carbohydrates of the Prokaryotic Cell* (London: Academic)
[17] Costerton J W, Ellis B, Lam K, Johnson F and Khoury A E 1994 Mechanism of electrical enhancement of efficacy of antibiotics in killing biofilm bacteria *Antimicrobial Agents Chemother.* **38** 2803–9
[18] Wellman N, Fortun S M and McLeod B R 1996 Bacterial biofilms and the bioelectric effect *Antimicrobial Agents Chemother.* **40** 2012–4
[19] Del Pozo J L, Rouse M S and Patel R 2008 Bioelectric effect and bacterial biofilms. A systematic review *Int. J. Artif. Organs* **31** 786–95
[20] Stoodley P, deBeer D and Lappin-Scott H M 1997 Influence of electric fields and ph on biofilm structure as related to the bioelectric effect *Antimicrobial Agents Chemother.* **41** 1876–9
[21] Del Pozo J L, Rouse M S, Mandrekar J N, Steckelberg J M and Patel R 2009 The electricidal effect: reduction of Staphylococcus and Pseudomonas biofilms by prolonged exposure to low-intensity electrical current *Antimicrobial Agents Chemother.* **53** 41–5
[22] Pareilleux A and Sicard N 1970 Lethal effects of electric current on *Escherichia coli Appl. Microbiol.* **19** 421–4
[23] Barranco S, Spadaro J, Berger T and Becker R 1974 *In vitro* effect of weak direct current on *Staphylococcus aureus Clin. Orthopaedics Relat. Res.* **100** 250–5

[24] Blenkinsopp S A, Khoury A and Costerton J 1992 Electrical enhancement of biocide efficacy against *Pseudomonas aeruginosa* biofilms *Appl. Environ. Microbiol.* **58** 3770–3
[25] Caubet R, Pedarros-Caubet F, Chu M, Freye E, de Belem Rodrigues M, Moreau J and Ellison W 2004 A radio frequency electric current enhances antibiotic efficacy against bacterial biofilms *Antimicrobial Agents Chemother.* **48** 4662–4
[26] Giladi M, Porat Y, Blatt A, Shmueli E, Wasserman Y, Kirson E D and Palti Y 2010 Microbial growth inhibition by alternating electric fields in mice with *Pseudomonas aeruginosa* lung infection *Antimicrobial Agents Chemother.* **54** 3212–8
[27] Bockris J O M and Reddy A K 2000 *Modern Electrochemistry* (New York: Kluwer Academic/Plenum)
[28] Kim Y W, Ben-Yoav H, Wu H C, Quan D, Carter K, Meyer M T, Bentley W E and Ghodssi R (ed) 2013 An enhanced bacterial biofilm treatment using superpositioned electric field *7th Int. Conf. on Microtechnologies in Medicine and Biology (MMB) (Marina del Rey, CA, 10–12 April 2013)*
[29] Kim Y W, Subramanian S, Gerasopoulos K, Ben-Yoav H, Wu H-C, Quan D, Carter K, Meyer M T, Bentley W E and Ghodssi R 2015 Effect of electrical energy on the efficacy of biofilm treatment using the bioelectric effect *npj Biofilms Microbiomes* **1** 15016
[30] Kumar A, Mortensen N P, Mukherjee P P, Retterer S T and Doktycz M J Electric field induced bacterial flocculation of enteroaggregative *Escherichia coli* 042 *Appl. Phys. Lett.* **98** 253701
[31] Kim Y W, Meyer M T, Berkovich A, Subramanian S, Iliadis A A, Bentley W E and Ghodssi R 2015 A surface acoustic wave biofilm sensor integrated with a treatment method based on the bioelectric effect *Sensors Actuators* A (in press)
[32] Mosteller M, Austin M, Ghodssi R and Yang S A 2014 Platforms for engineering biomedical experiments *IEEE Syst. J.* **9** 1218–28
[33] Ceri H, Olson M E, Stremick C, Read R R, Morck D and Buret A 1999 The calgary biofilm device: new technology for rapid determination of antibiotic susceptibilities of bacterial biofilms *J. Clin. Microbiol.* **37** 1771–6
[34] Weibel D B, DiLuzio W R and Whitesides G M 2007 Microfabrication meets microbiology *Nat. Rev. Microbiol.* **5** 209–18
[35] Whitesides G M, Ostuni E, Takayama S, Jiang X and Ingber D E 2001 Soft lithography in biology and biochemistry *Annu. Rev. Biomed. Eng.* **3** 335–73
[36] Kim J, Hegde M, Kim S H, Wood T K and Jayaraman A 2012 A microfluidic device for high throughput bacterial biofilm studies *Lab Chip* **12** 1157–63
[37] Kim K P, Kim Y-G, Choi C-H, Kim H-E, Lee S-H, Chang W-S and Lee C-S 2010 *In situ* monitoring of antibiotic susceptibility of bacterial biofilms in a microfluidic device *Lab Chip* **10** 3296–9
[38] De Man J C, Rogosa M and Sharpe M E 1960 A medium for the cultivation of lactobacilli *J. Appl. Bacteriol.* **23** 130–5
[39] Bakke R, Kommedal R and Kalvenes S 2001 Quantification of biofilm accumulation by an optical approach *J. Microbiol. Methods* **44** 13–26
[40] Bakke R and Olsson P 1986 Biofilm thickness measurements by light microscopy *J. Microbiol. Methods* **5** 93–8
[41] Meyer M T, Roy V, Bentley W E and Ghodssi R 2011 Development and validation of a microfluidic reactor for biofilm monitoring via optical methods *J. Micromech. Microeng.* **21** 054023
[42] Paliy O and Gunasekera T S 2007 Growth of *E. coli* bl21 in minimal media with different gluconeogenic carbon sources and salt contents *Appl. Microbiol. Biotechnol.* **73** 1169–72
[43] Yang X, Beyenal H, Harkin G and Lewandowski Z 2000 Quantifying biofilm structure using image analysis *J. Microbiol. Methods* **39** 109–19
[44] Whitesides G M 2006 The origins and the future of microfluidics *Nature* **442** 368–73
[45] Kim Y W, Sardari S E, Meyer M T, Iliadis A A, Wu H C, Bentley W E and Ghodssi R 2012 An ald aluminum oxide passivated surface acoustic wave sensor for early biofilm detection *Sensors Actuators* B **163** 136–45
[46] Subramanian S, Gerasopoulos K, Sintim H O, Bentley W E and Reza G 2015 A bacterial biofilm combination treatment using a real-time microfluidic platform *18th Int. Conf. on Solid-State Sensors, Actuators and Microsystems (Transducers '15) (Anchorage, Alaska, 21–25 June 2015)* pp 2216–9
[47] Meyer M T, Subramanian S, Kim Y W, Ben-Yoav H, Gnerlich M, Gerasopoulos K, Bentley W E and Ghodssi R 2015 Multi-depth valved microfluidics for biofilm segmentation *J. Micromech. Microeng.* **25** 095003